American Welding Society®

SUPPLEMENT TO THE *WELDING JOURNAL*, FEBRUARY 2022
Sponsored by the American Welding Society

WELDING RESEARCH

# Investigation and Optimization of Resistance Implant Welding of Polypropylene Sheets

## The effects of wire geometries and wire diameters on the characteristics of polypropylene sheets united by resistance implant welding were examined

BY H. BAKIRCI, İ. KARAGÖZ, AND M. A. KAYA

## Abstract

Recently, the use of resistance welding in the joining of polymeric materials and polymer composites in the aviation, marine, and automotive industries has been gradually increasing. However, challenges continue in regard to improving product quality as affected by several parameters. This study focused on the effects of wire geometries and wire diameters on the characteristics of polypropylene (PP) sheets united by resistance implant welding. Here, PP sheets manufactured by the injection molding method were joined via the resistance upset welding method with three different wire geometries, including spiral, wavy, and M-shaped, and two different wire diameters of 0.3 and 0.5 mm. Mechanical properties, morphological properties, and heating characteristics were examined. The results showed that wire diameter and wire geometry affected amount of heat formation in the weld zone and, therefore, weld performance in terms of the mechanical properties. The results obtained from the study can be used as a reference in similar applications.

## Keywords

- Resistance Upset Welding
- Plastic Joining
- Welding Performance
- Resistance Welding
- Plastic Welding

*https://doi.org/10.29391/2022.101.004*

## Introduction

Different welding methods have been developed for thermoplastic materials by simply adapting metal welding techniques to plastics. They might vary by the purpose of use and the application area. Electric resistance welding (RW), which was formerly used for the welding of metallic sheets and plate-type materials, is one of the metal welding methods tailored to welding thermoplastics. In many sectors, such as automotive, aeronautics and space, electrical and electronics, construction and machinery manufacturing, etc., thin-sectioned metal materials undergo deformation under a high temperature during the RW process. To prevent deformation, the welding of thin-sectioned materials should be performed at low temperatures and in short periods of time (Ref. 1). Electric RW is highly preferred for fast welding with the least possible deformation and for an economical and high-strength joining process (Ref. 2). The heat required in RW is provided by the contact resistance of these materials against the electric current passing through the metal material. In the welding process, the sections to be welded in parts are partially melted by this heat to create a weld pool. After the weld pool is formed, the electric current passing through the parts is cut off, and pressure is applied to the parts by means of electrodes or jaws in the welding machine until the workpiece cools and solidifies (Refs. 3, 4). The low voltage required for electric RW and the high-current electrical power are provided by welding transformers (Ref. 5).

Since plastic materials are insulating (they do not conduct electricity), to obtain the heat required for welding thermoplastics by this method, a metallic material must be inserted between two plastic materials through which the electric current will pass. Due to this implant inserted between two plastic materials, RW is also called resistance implant welding (RIW) or electrofusion welding (EFW) for plastics (Refs. 6, 7). The application of RIW to thermoplastics is shown in Fig. 1. Unlike RW, the application of RIW to thermoplastics is carried out in three stages. At the first stage

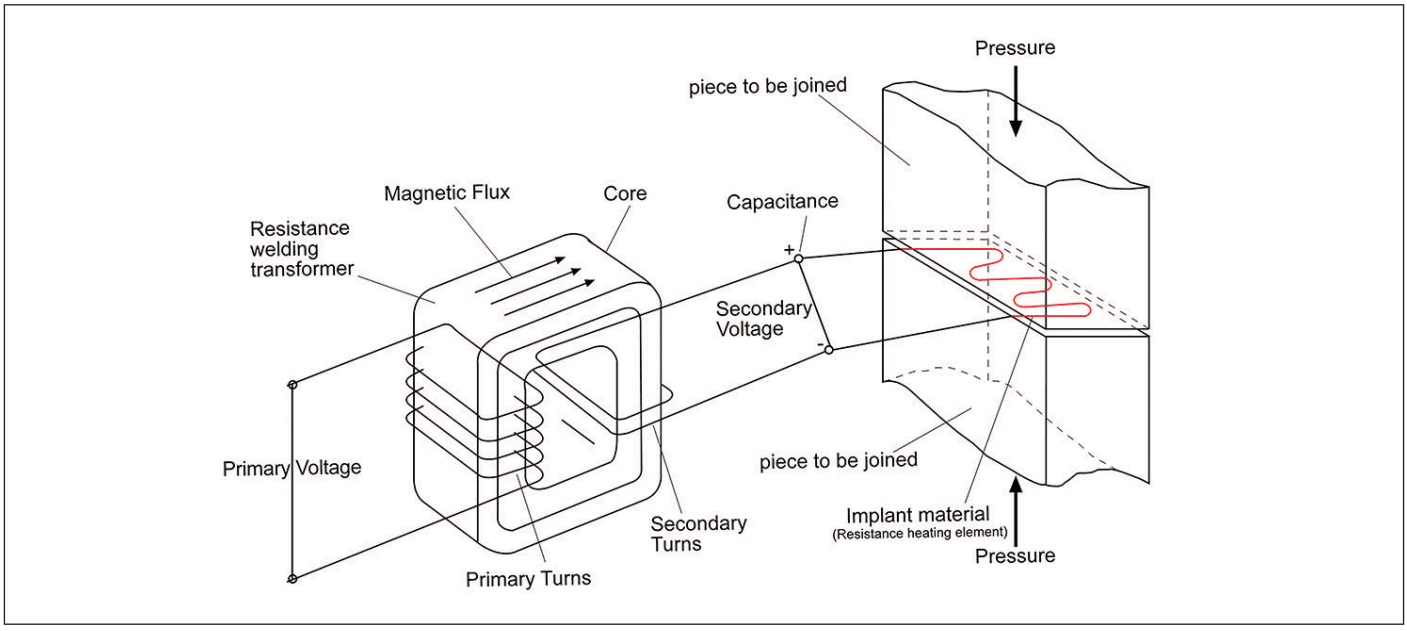


*Fig. 1 — The schematic diagram of the resistance implant welding process.*

(assembly stage), the implant (usually a wire) is placed between the parts to be joined. At the second stage, the area to be joined is heated by passing an electric current through these wires. The plastic around the wire, which is heated via thermal conduction of the implant materials, melts and provides the fluidity required for joining. At the end of the heating temperature and heating time, which vary according to the type of material, the current is cut off, and pressure is applied to the parts for joining. At the last stage, the welding process is completed by cooling the plastic that was melted under pressure. In this method, the metal wires used as heating elements are left in the weld zone. This might result in extra strength, but they are left because they cannot be easily removed (Refs. 6–11).

The RIW method is mainly focused on joining thermoplastics reinforced with various continuous fibers (Ref. 12), such as carbon fiber (Ref. 9) and glass fiber (Refs. 13, 14). Recently, the RIW process has been utilized in special fields that need strict performance requirements, such as aerospace (Ref. 15), automotive (Ref. 16), electronic (Ref. 17), and composite applications, and also have special advantages applicable to complex-shaped parts, easy operation, and low-cost equipment (Refs. 17, 18). For example, the leading edges of the wings of the Airbus A340-600 and A380 are assembled by RIW (Ref. 19). In addition, RW has also been employed for boat and vessel production (Ref. 17), plastic pipe and fittings joining (Ref. 20), two-parted bumpers, and automotive body panel assembling (Ref. 16).

Electrically resistive implant materials play a key role in RW (Ref. 21). As the electrical current passes through, the heated implant material provides the heat needed for melting polymer surfaces, and then joining can be carried out with the applied pressure (Ref. 22). Carbon fibers, graphite woven textiles, steel knitted meshes, and nickel-chromium alloy (Ni-Cr) wires are examples of implant materials for RW processes (Ref. 16).

Ni-Cr wires are generally preferred as a heating implant material to prevent the weld strength from decreasing in the weld zone because of corrosion. To prevent a decrease in weld strength due to corrosion, Starrov and Bersee (Ref. 14) used a networked heating element made of carbon fiber and achieved 10–20% improvement. For the same purpose, Warren et al. (Ref. 22) utilized a polymeric film in the joining interface. They reported that by employing the polymer film in the weld zone, the openings in the wire mesh decreased. Thus, some voids in the joining area can be filled at even low application pressures; hence, the weakening of weld strength due to corrosion can be precluded. They also declared that the wire material, wire diameter, and wire geometry strictly affect the weld strength.

O'Shaughnessey et al. (Ref. 19) reported that weld strengths were strictly affected by polymer type, part dimension, and the shape of implant materials and also stated that RW provides better heat dissipation in the weld area compared to ultrasound and induction welding (IW) methods. Dubé et al. (Ref. 23) determined that the mechanical performance of the welded joint increases and the delamination problem can be avoided when a surface treatment, such as $TiO_2$, and polymer coating are applied to the implant materials. They also concluded that joining with RW in thermoplastic composites, such as carbon fiber/polyetheretherketone, carbon fiber/polyetherketoneketone, carbon fiber/polyetherimide, and woven glass fiber/polyetherimide, is more advantageous than joining with adhesive.

Shi et al. (Ref. 24) stated that good contact of the material surfaces to be joined prevents the formation of microcracks, insufficient heating time affects the root penetration and decreases the weld strength, and correct adjustment of the welding pressure ensures contact with the weld interface and prevents the formation of joint clearances.

Starrov and Bersee (Ref. 14) observed that the cooling rate after welding is an effective parameter on the crystallization degree, which is an important issue for weld strength and weldability in their studies for the aviation industry. Depending on the cooling rate, cooling can be isothermal or nonisothermal. Isothermal

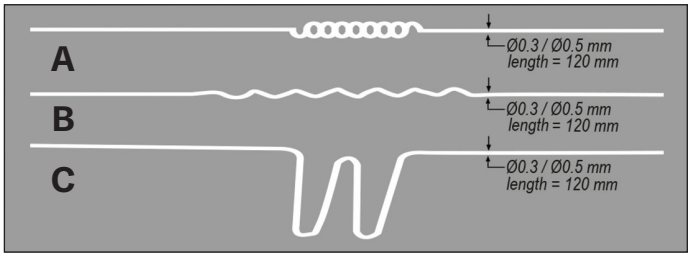


*Fig. 2 — Shapes of joining materials: A — Spiral; B — wavy; C — M-shaped.*

cooling is typical for low power levels and can provide process conditions that are able to reduce residual stresses. On the other hand, due to its high power levels, nonisothermal cooling can cause undesired stress and distortion in weld areas. For moderate power levels, cooling is not isothermal but is close to the recommended processing temperature of the material and provides an acceptable crystallinity.

In terms of weld performance, resistance values of the implant material and heat transfer (Ref. 25), heating time (Refs. 24, 26), application temperature (Ref. 17), geometries and diameters of the implant material (Refs. 22, 24, 27), and joining angle and welding pressure (Refs. 17, 28) are stated to be vital parameters. The RW method can provide more even temperature distribution in comparison to other welding processes. It is also known that the obtained weld performance is strictly dependent on the temperature's correct adjustment in the weld zone (Ref. 29).

There are a limited number of studies regarding RIW (Ref. 12). These studies were generally about employing RIW for joining thermoplastic composites materials (reinforced with various fibers, such as glass fiber or carbon fiber) via carbon fiber and stainless steel mesh as implant materials. Also, it can be said that RIW methods were utilized only as lap welding and evaluated only for lap shear strength values of joining parts.

Our work was aimed to perform a RIW method as upset welding of neat polymeric materials that do not contain any additives or reinforcement materials and evaluate the performances of the joining in terms of various mechanical perspectives. As known, especially in repair and maintenance applications, upset welding has important application areas, as it provides the opportunity to combine without disrupting the part geometry. These applications are frequently practiced in many industrial branches because of their simplicity and low-cost characteristics. The principal requirements of applications should be referred to as universality, ease, and cost effectiveness.

In this study, the butt joint method was applied on neat polypropylene (PP) sheets, which cannot be easily joined using adhesive and have a wide range of uses in many industrial sectors (Ref. 30) via wire-based implant materials. Welding processes were varied by changing the essential parameters, such as welding angle, implant material (wire) diameter, and geometry. Welding performances of samples were evaluated not only with tensile strength and modulus values but also with various test results, namely flexural strength, flexural modulus, impact strength, impact modulus, morphological examination, and heating characteristics. The obtained results were presented with consideration to the parameters, and ultimately the optimization of the welding performances was completed within the framework of these parameters.

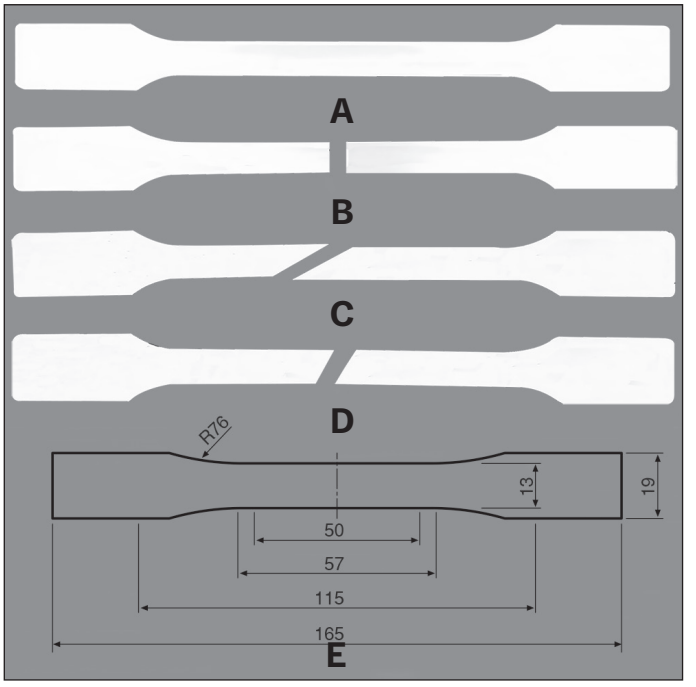


*Fig. 3 — Samples: A — Reference; B — cut at 90-deg angle; C — cut at 30-deg angle; D — cut at 45-deg angle; E — dimensions of specimen (ASTM D638 Type I).*

## Materials and Methods

### Materials

In this study, Isplen® PP 070 G2M, trade coded PP produced by Repsol, was chosen as the polymeric material used in the joining process. The essential properties of PP are shown in Table 1.

Ni-Cr wires with diameter values of 0.3 and 0.5 mm were used as resistance implant materials. To evaluate the effects of the wires' geometry on the joining performance, wires were also formed into different shapes (spiral, wavy, and M-shaped), as seen in Fig. 2. Special apparatuses were used in the wire-forming process to obtain uniform implant joining materials. It is important to note that the length of the joining materials was 12 cm and was the same for all shapes.

### Methods

Test specimens were prepared in compliance with ASTM D638, *Standard Test Method for Tensile Properties of Plastics*, from PP polymeric materials via the ENGEL Victory 80 plastic injection machine, which has 800 kN of clamp force. Specimens were cut in half at different angles using the Proxxon Bench Circular Saw machine for upset welding. Figure 3 shows the specimens cut in 90-, 30-, and 45-deg angles.

After the cutting procedure, pieces were joined using RW. In this method, a 12 Vmax/50 Wmax power supply was utilized to energize the heating elements. Fluctuations in the resistance of heating elements due to elevated temperature (resistance increases as the temperature raises) were compensated with a

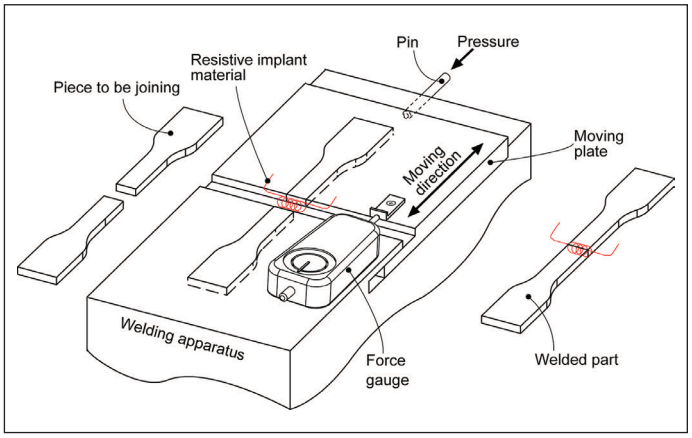


*Fig. 4 — Special template for using specimen welding.*

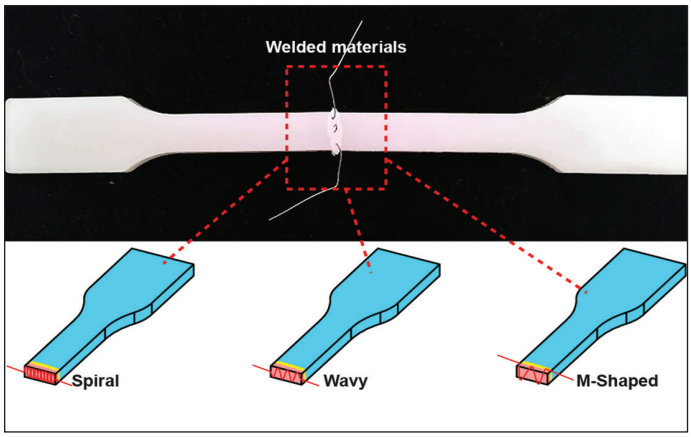


*Fig. 5 — Welded part view after RIW joining.*

**Table 1 — The Properties of Isplen PP 070 G2M**

| Properties | Typical Value | Unit | Test Method |
|---|---|---|---|
| Melt flow index (230°C/2.16 kg) | 12 | g/10 min | ASTM D1238 |
| Density (23°C) | 0.905 | $g/cm^3$ | ASTM D1505 |
| Hardness (23°C) | 68 | Shore D | ASTM D2240 |

potentiometer connected in series to the heating element. By changing the value of the potentiometer, we ensured the voltage across the heating element was constant (4.10 V). It is known that the resistance of a material is calculated by the following formula:

$$R = \frac{pL}{A} \quad (1)$$

where p is the resistivity of a given material, L is the length, and A is the cross-sectional area of the material.

In this study, the same type of materials (Ni-Cr) were used in a specific length, and, therefore, the resistivity and length values in Formula 1 were constant, but the A in the denominator changed based on the wire diameter. As the cross-sectional area ($\pi r^2$) is proportional to the $r^2$, the 0.3-mm-diameter wire had 2.77 times higher resistance compared to the 0.5-mm-diameter wire. It is known that heat is generated by joule in the heating elements and is proportional to the power dissipation in the wire. Since power can be calculated as

$$P = \frac{V^2}{R} \quad (2)$$

where V is the voltage across the heating element and R is the resistance of the same element, it is obvious that the heating element with a 0.5-mm-diameter wire can provide 2.77 times more heat energy than the 0.3-mm-diameter wire as the voltage for both elements is kept constant during the welding process. Since thicker wire can provide more heat energy, the required temperature in the welding process can be reached in a shorter time.

The welding process took place in an apparatus, seen in Fig. 4, equipped with an INSIZE push/pull force gauge measuring the applied force (max. 10 N) and guiding us to join specimen halves uniformly and homogeneously. Throughout this manuscript, the specimens are named using abbreviations to indicate the specifications more easily and efficiently. The material codes are designated as wire shape (S/spiral, W/wavy, or M/M-shaped), cutting angle (30, 45, or 90 deg), and wire thickness (0.3 or 0.5 mm). As an example, S3003 indicates a specimen with a spiral-shape wire, cutting angle of 30 deg, and a wire thickness of 0.3 mm. Figure 5 shows the welded part view after RIW joining.

## Characterizations

Tensile test specimens and cut-then-welded ones were evaluated through their tensile and flexural properties. Tensile tests and flexural tests were conducted using a ZwickRoell Z020 universal testing machine with a 20-kN load cell. The tensile test was conducted according to ASTM D638 and performed at room temperature at a drawing rate of 50 mm/min. The flexural test was performed based on ISO 178:2019 (en), *Plastics — Determination of flexural properties*, and the test was performed at room temperature and at a flexural rate of 2 mm/min. An Izod impact test was performed using an Instron CEAST 9050 machine (with a 5.5-J hammer) according to ISO 180:2019, *Plastics — Determina-*

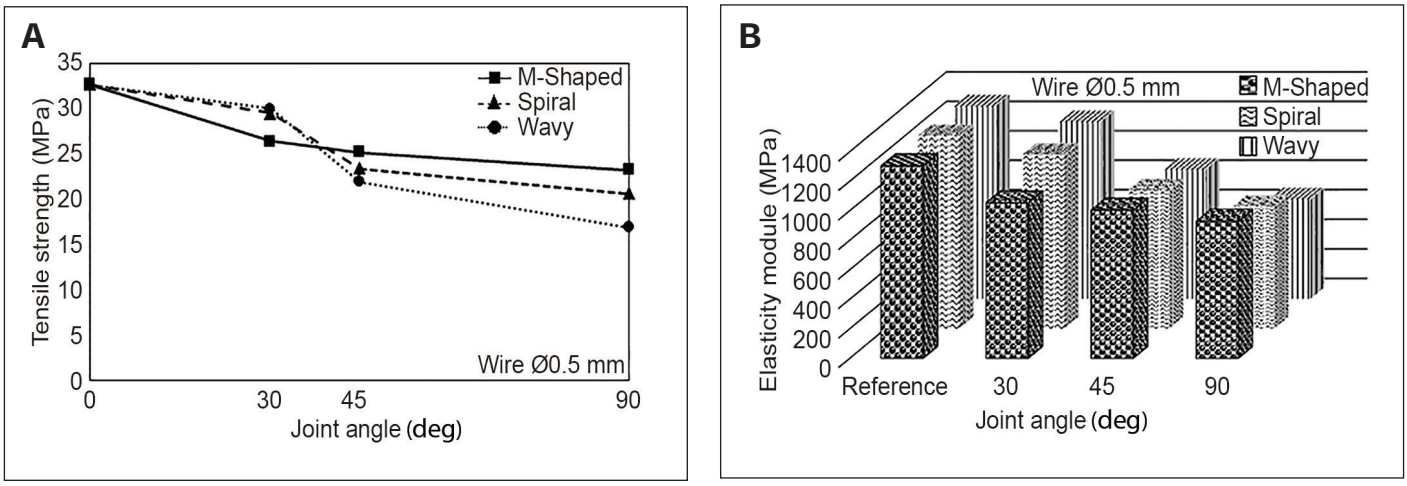


*Fig. 6 — Comparison of (A) tensile strength and (B) elasticity modules according to the wire geometry and joining angle of the 0.5-mm wire diameter.*

**Table 2 — Tensile Test Results**

| Sample Code | Tensile Strength (MPa) | Tensile Modulus (MPa) | Standard Deviation |
|---|---|---|---|
| Reference | 32.64 | 1305 | 0.02 |
| S3003 | 20.63 | 825 | 0.45 |
| S4503 | 20.45 | 818 | 0.41 |
| S9003 | 10.73 | 430 | 1.45 |
| S3005 | 29.47 | 1179 | 0.18 |
| S4505 | 23.37 | 935 | 0.85 |
| S9005 | 20.62 | 825 | 0.25 |
| W3003 | 25.15 | 1006 | 0.29 |
| W4503 | 18.97 | 759 | 0.84 |
| W9003 | 8.78 | 351 | 1.65 |
| W3005 | 29.69 | 1198 | 0.15 |
| W4505 | 21.88 | 875 | 0.35 |
| W9005 | 16.86 | 675 | 1.25 |
| M3003 | 24.33 | 973 | 0.45 |
| M4503 | 19.46 | 779 | 0.65 |
| M9003 | 18.20 | 728 | 0.95 |
| M3005 | 26.35 | 1054 | 0.45 |
| M4505 | 25.14 | 1005 | 0.35 |
| M9005 | 23.20 | 928 | 0.25 |

*tion of Izod impact strength*. For each test, at least five specimens were used. The morphological examination of welded specimens was carried out using an Olympus BX51M optical microscope at 400× magnification. Heating characteristics, such as spread and rate, of weld surfaces were also monitored by the FLIR E8 infrared camera while the welding process was taking place.

## Results

### Results of Tensile Tests

The tensile strength ($\sigma_M$), modulus of elasticity (Em), and performance values of welded specimens compared to the unprocessed specimen are given in Table 2 and Figs. 6 and 7.

The tensile strength values are compared to the 0.5-mm-diameter wire in Fig. 6A and the 0.3-mm-diameter wire in Fig. 7A, and the moduli of tensile elasticity is compared to the 0.5-mm-diameter wire in Fig. 6B and the 0.3-mm-diameter wire in Fig. 7B.

### Results of Flexural Tests

The results of the flexural tests can be seen in Table 3. The comparison of flexural strength ($\sigma_{FC}$) and flexural modulus ($E_F$) according to the wire diameter and joining angle are given in Fig. 8. A comparison of the bending strength in Fig. 8A, the modulus of bending elasticity in Fig. 8B according to the wire diameter and joining angle, and the weld performance in Fig. 8C according to bending strength was performed.

### Results of Impact Tests

The results from the impact strength tests are shown in Table 4. The comparison of impact strength and weld performance according to the wire diameter and joining angle is given in Fig. 9.

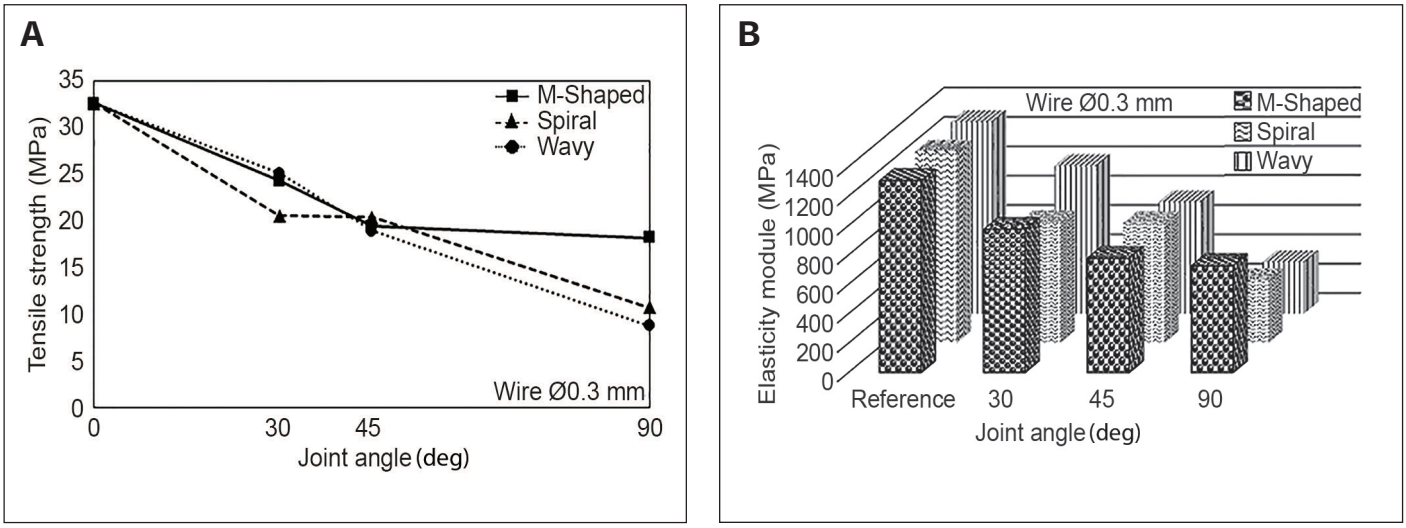


*Fig. 7 — Comparison of (A) tensile strength and (B) elasticity modules according to the wire geometry and joining angle for the 0.3-mm-diameter wire.*

## Results of Morphological Examinations and Heating Characteristics of Welding Surfaces

Images obtained from morphological examinations are shown in Fig. 10. Thermal camera images are shown in Fig. 11.

# Discussion

## Tensile Tests

When the values in Table 2 are examined, it is observed that the mechanical properties of the weld weakened as the joining angle increased. This shows that the surface area of the joint was strictly related to weld strength values. As the joining angle decreased, the surface area in the joint zone increased, thus increasing the tensile strength values. Also, plastic welds are always weakest in peel then tension then shear. This is also why most structural applications are designed to put the weld in shear. The highest tensile strength values were obtained from the joining process at the 30-deg angle, and a downward trend in tensile strength values was observed with an increased joining angle. In the study conducted by Hagglund et al. (Ref. 31), the same trend was observed and the results matched quite well with our findings. Higher weld strength values can be reached by adjusting the weld angle and geometry of implant materials, which can reduce defects like openings in welding areas.

As can be seen in Figs. 6 and 7, tensile strength (Figs. 6A, 7A) and the modulus of tensile elasticity (Figs. 6B, 7B) decreased as the joining angle increased. In both wire thicknesses, as the joining angle increased, the M-shaped wire geometry displayed better behavior than the others. This is thought to be due to the fact that the melt flow in the weld zone with the increasing angle is guided by the wire geometry and provides better root penetration around the wire. This will be better understood when considered together with the melt flow in the weld zone.

It was also determined that in terms of wire thickness, the weld performance, according to both tensile strength and modulus, was affected. To achieve a better weld performance, the 0.5-mm-diameter wire should be chosen, as can be seen in Figs. 6 and 7, because the weld performance is directly related to the amount of current. Using a thicker wire implant (for our study, 0.5 mm), the melting process can be performed more effectively and rapidly, thus better weld performance values can be reached.

## Flexural Tests

The flexural strength values of the welded materials (Table 3) were very close to the flexural strength values of the intact material. There was no breakage observed in the samples. Similar to the tendency observed in the tensile tests, the flexural strength values decreased while the joining angle increased. Contrary to this situation, the increase (Fig. 8) in the value of the M9005 sample is thought to be caused by an exceptional experimental error. The flexural strength values increased as the joining angle reduced, and the wire geometry changed from M-shaped to spiral and finally to wavy. The highest flexural strength was obtained when the joining angle and wire geometry were 30 deg and wavy.

## Impact Tests

When the results that are given in Table 4 and Fig. 9 are examined in terms of wire geometry, it is seen that the highest impact strength values were obtained from the samples using wire with a spiral geometry. Since the wire with the spiral geometry had a more effective root penetration characteristic in the weld areas during the welding process compared to the wires with wavy and M-shaped geometries, the welded samples with spiral-formed wires resisted higher impact values.

The welding wire geometry and wire diameter have an effect on method selection and weld performance. It has been known that the amount of heat in the weld areas can vary depending on the wire thickness and amount of electrical current (Refs. 3, 10,

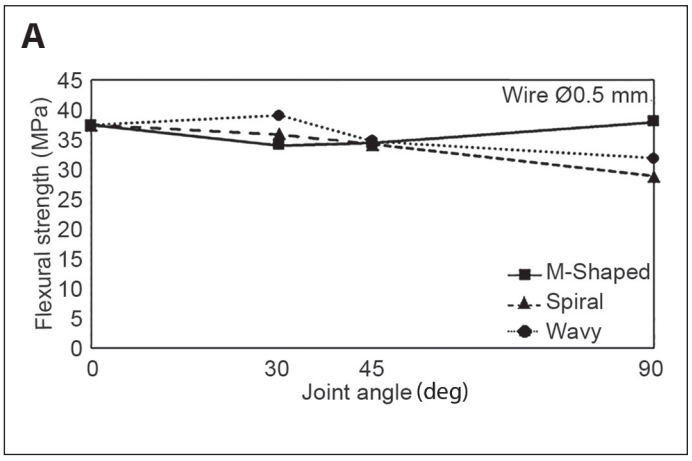


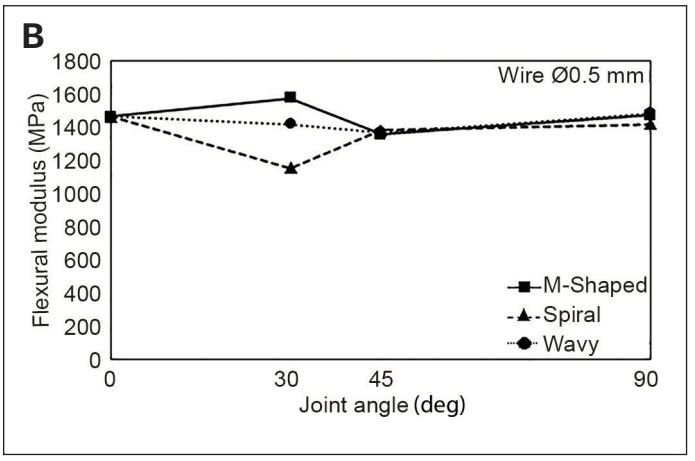


**Table 3 — Flexural Test Results**

| Sample Code | Tensile Strength (MPa) | Tensile Modulus (MPa) | Standard Deviation |
|---|---|---|---|
| Reference | 37.41 | 1461 | 0.03 |
| S3005 | 35.87 | 1150 | 0.14 |
| S4505 | 34.13 | 1380 | 0.32 |
| S9005 | 28.88 | 1415 | 0.28 |
| W3005 | 39.07 | 1417 | 0.38 |
| W4505 | 34.80 | 1366 | 0.18 |
| W9005 | 31.80 | 1483 | 0.23 |
| M3005 | 34.35 | 1575 | 0.25 |
| M4505 | 34.05 | 1354 | 0.18 |
| M9005 | 37.98 | 1472 | 0.12 |

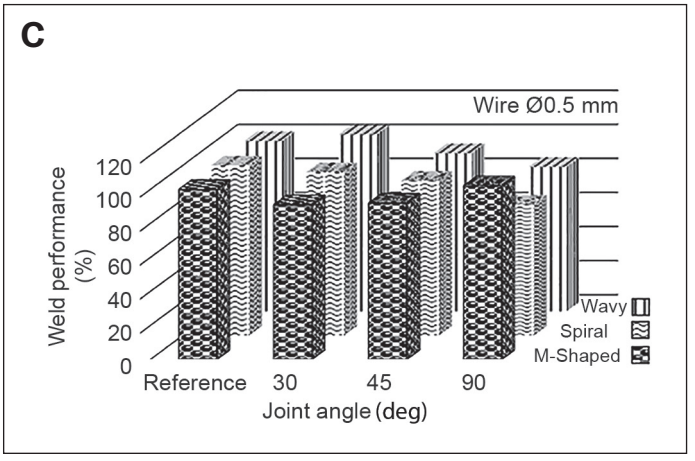


*Fig. 8 — For the 0.5-mm-diameter wire, comparison of (A) flexural strength, (B) flexural module, and (C) weld performance values according to the wire geometry and the joining angle.*

32). Generated heat flow can be easily controlled by changing these two parameters. Thus, the depth of the root penetration of the implant materials in the weld areas can be obtained at desired levels, and this ensures better weld strength. Employing smaller wire diameters in the weld areas causes insufficient heat, lowering root penetration levels of implant materials and, as a result, decreasing weld strength values. This matches with the explanation given in the Materials and Methods section.

When the results are evaluated in terms of the joining angle, it is seen that the best results were obtained from the welding processes performed at 30 deg. This situation is thought to be caused by the slope. As the slope changed the surface area, additional impact strength occurred and increased the total impact strength in parallel.

## Morphological Examinations

In microstructure studies, color changes due to heat were encountered in welded wires. Flow traces, fluctuations, and, rarely, wire oxidation occurring in the material from the effect of heat were clearly seen in the weld area — Fig. 10. In the circumference of the wire, a few small openings were observed directly in the melt flow direction. Voids formed during the welding process can cause oxidation (Ref. 14). Reducing the openings with the correct selection of the welding angle, wire diameter, geometry, and material of the heating element will greatly prevent oxidation. In this study, it was seen that as the wire geometry changed, the formation of the openings decreased, fluctuation in the welding area changed direction, and oxidation decreased depending on heat flow. Additionally, the flow direction of the molten plastic in the weld zone was affected by the heat characteristic in the weld zone as well as the wire geometry. The pressure applied during

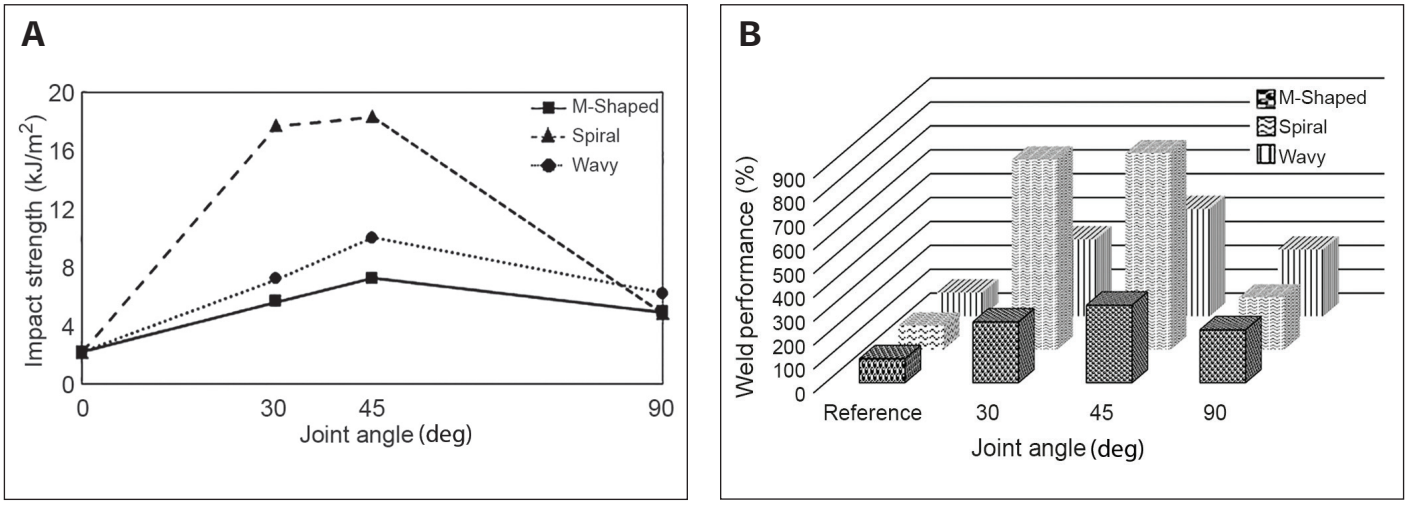


*Fig. 9 — Comparison of impact test results of different wire geometries for the 0.5-mm-diameter wire: A — Impact strength; B — weld performance.*

**Table 4 — Impact Test Results**

| Sample Code | Impact Strength (kJ/m²) | Standard Deviation |
|---|---|---|
| Reference | 2.23 | 0.15 |
| S3005 | 17.73 | 0.56 |
| S4505 | 18.32 | 0.35 |
| S9005 | 4.86 | 0.52 |
| W3005 | 7.19 | 0.45 |
| W4505 | 10.03 | 0.42 |
| W9005 | 6.24 | 0.63 |
| M3005 | 5.67 | 0.65 |
| M4505 | 7.23 | 0.25 |
| M9005 | 4.93 | 1.10 |

welding also had an effect on the formation of voids in the microstructure. The material flowed out of the weld zone under high pressure, and if the pressure was too low, the number of openings increased since there was no adequate pressure that ensured a homogeneous distribution of the molten material in the weld zone. Until the welded joint cools down, a steady application of pressure will significantly reduce the formation of voids (Ref. 7).

In terms of microstructure, it was seen in all the welds that the molten polymer wrapped the welding wire like a thin film and created a transition zone between the polymeric material and the wire. A similar structure at the interface between the wire and the polymeric material and applying a surface treatment to the wire would increase the weld performance. The treatment of the wire surface by polymeric film or $TiO_2$ coating can make the surface compatible with the material (Refs. 21, 33).

## Heating Characteristics of Welding Surfaces

It was determined that when the temperature in the weld zone was low, the material did not melt completely and there was not enough root penetration for welding. In the case of a high temperature, the material burned due to overheating.

In thermal camera examinations (Fig. 11), it was also seen that at temperatures close to the melting temperature (Tm) of polymer, the heat was homogeneously distributed in the entire welding area, and sufficient root penetration was obtained for joining. Wire diameter and the heating energy used affected heat generation and root penetration in the weld zone because the heat obtained in the weld area differed according to the wire diameter (Ref. 34). The heat generated by the various wire diameters of the same type of materials in same lengths supports this statement. For this reason, a proper wire diameter should be chosen, as it affects the provided heat energy in reaching a desired temperature close to the melting temperature of the joining polymer materials. In our study, the optimum working temperature of the PP material for RW was determined as 217°C, and the heating time was determined as 13 s. It is noteworthy that the wire with the larger cross-sectional area provided more heat and, therefore, reached the optimum temperature in a shorter time. A 0.5-mm-diameter heating element reached 217°C in 13 s, and, therefore, that is the time we should keep for the welding process to get the best results under the given specifications. It is important to point out that the temperature was not steady during the welding procedure. In contrast, the temperature kept increasing, surging the procedure,

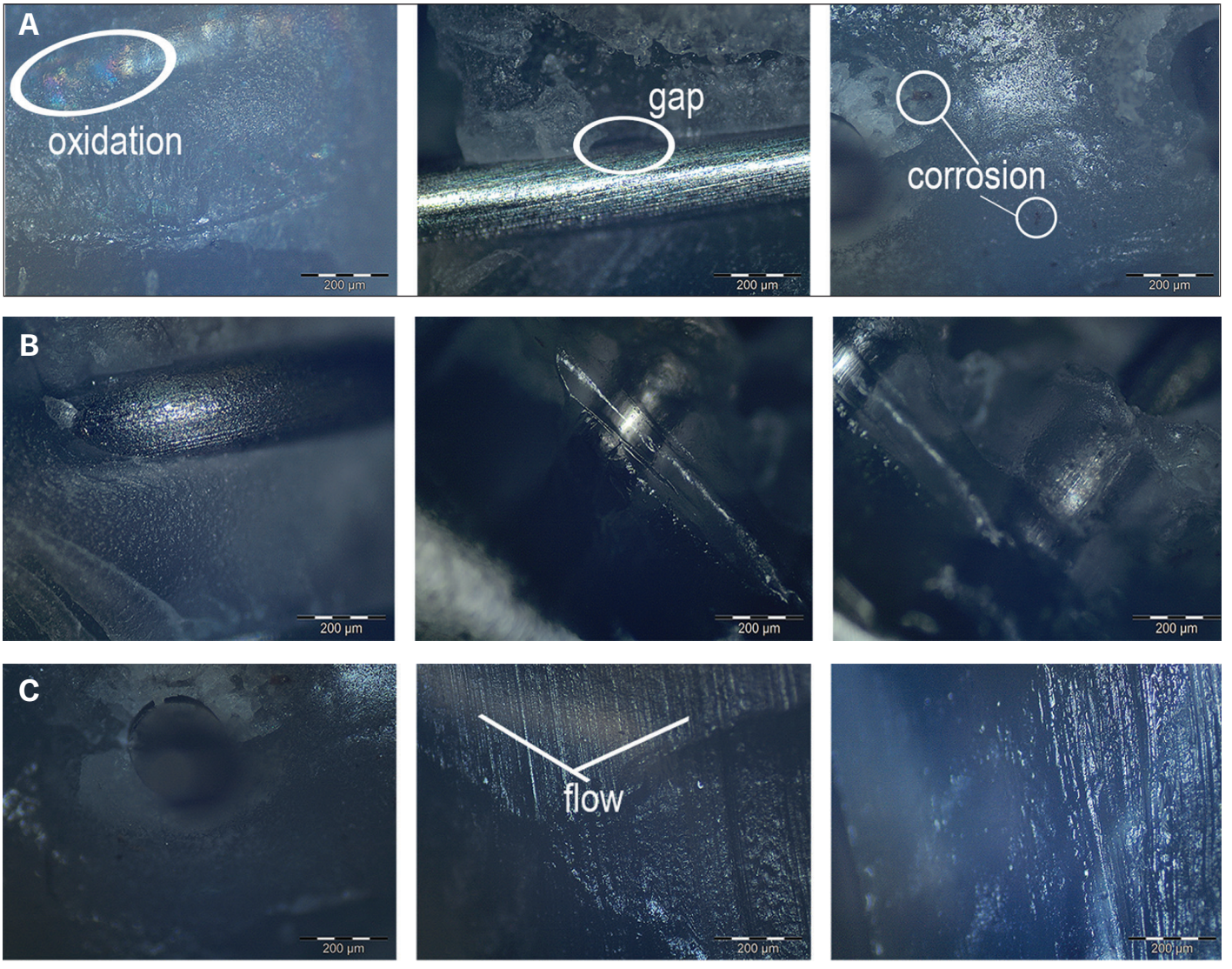


*Fig. 10 — Optical microscope images of welded materials: A — Spiral; B — wavy; C — M-shaped.*

and when the temperature reached 217°C in 13 s, the process was terminated, giving the best weld results. The welding range between 210 and 250°C is known to give the best results for PP joining (Ref. 30).

## Conclusions

In this study, PP sheets were successfully joined via RW at an angle of 30, 45, and 90 deg using Ni-Cr wires that were 0.3 and 0.5 mm in diameter and had spiral, wavy, and M-shaped geometries. The main results obtained from this study can be summarized as follows:

1) Higher weld performance values can be achieved easily by using optimized parameters figured from the results of tensile, flexural, and impact tests.

2) The welding wire diameter influences heat generation in the weld zone. In the study, as the wire thickness increased, the heat input into the weld zone increased, thus creating the ideal joining heat for the weld zone. In the joints made with wires with lower cross sections, oxidation occurred in the weld zone.

3) Wire geometry is important for the joining process. In the welding operations, the root penetration in the weld zone made from wire with a spiral geometry was higher than with other geometries. The tensile strength, bending strength, and impact strength of the materials varied depending on the wire geometry.

4) With the pressure applied during joining, the wire geometry directed the melting flow in the weld zone. Depending on the geometry of the wire and the direction of the flow, it was determined that gaps are formed at the points where the cross section is narrow. These openings have a notch effect and a negative impact on the weld strength.

5) The joining temperature has a significant effect on weld strength. Joints made at temperatures below and close to melting temperatures provide the required root penetration to gain maximum performance from the joining process.

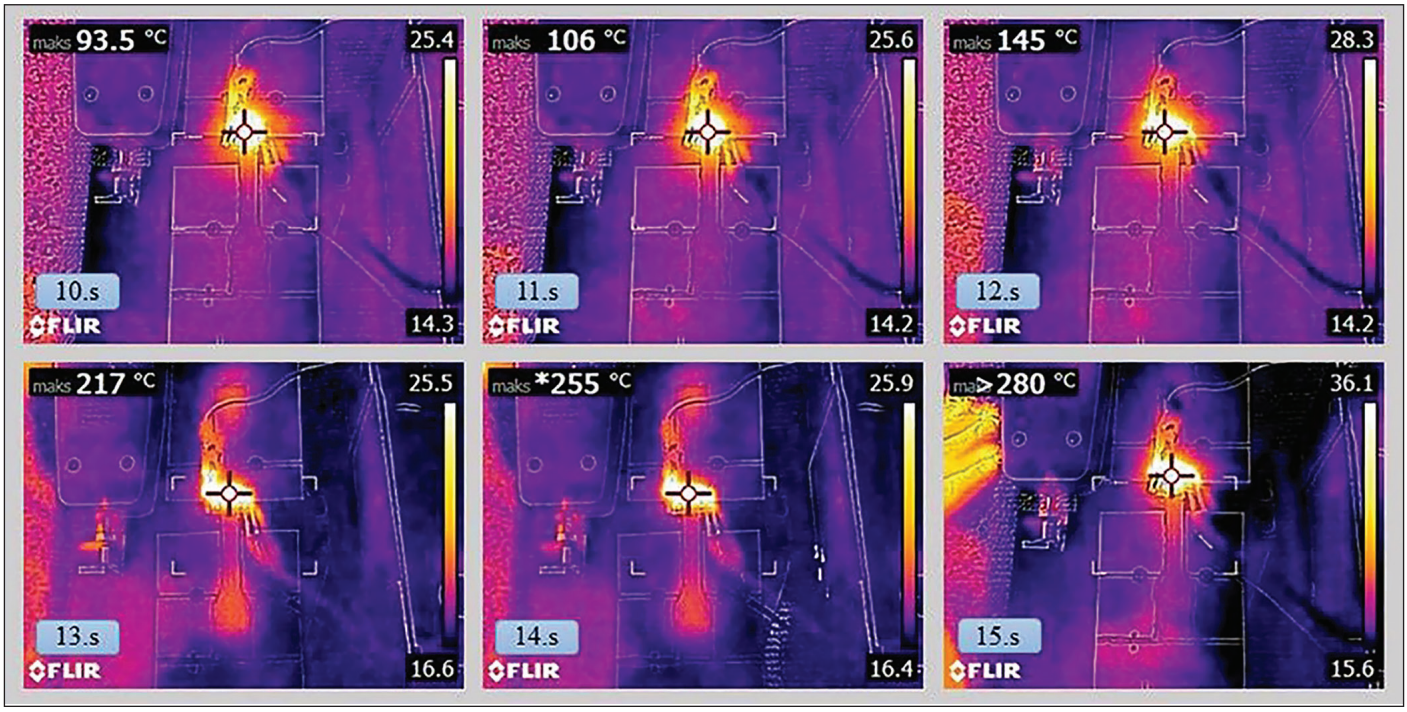


*Fig. 11 — Thermal infrared (IR) camera images of welded materials.*

6) Consequently, to achieve the best resistance upset welding performance for neat PP sheets, optimized process parameter values might be utilized. The following summarizes the best parameters we have revealed in this study. When the diameter of the wire is 0.5 mm, geometry of the wire is spiral, welding temperature is 217°C, heating time is 13 s, applying pressure is 10 N, and the joining angle is 30 deg, the best weld performance for PP sheets can be achieved.

## *Acknowledgment*

The authors gratefully acknowledge the financial support (Project Nos. 2018/AP/0014 and 2018/YL/0024) of the Yalova University Scientific Research Projects Coordination Unit, Yalova, Turkey.

## *References*

1. Wang, H., Wagner, S., Sekol, R., Chen, N., Perry, T., and Schroth, J. 2020. Resistive joining — A novel dissimilar welding method for thin sheet metals. *Procedia Manuf.* 48: 141–146. DOI: 10.1016/j.promfg.2020.05.030

2. Araújo, I. G., Santos, L. F., Marques, L. F. B., Reis, J. F., Souza, S. D. B., and Botelho, E. C. 2019. Influence of environmental effect on thermal and mechanical properties of welded PPS/carbon fiber laminates. *Mater. Res. Express.* DOI: 10.1088/2053-1591/ab3acd

3. Iatcheva, I., Darzhanova, D., and Manilova, M. 2018. Modeling of electric and heat processes in spot resistance welding of cross-wire steel bars. *Open Phys*. 16(1): 1–8. DOI: 10.1515/phys-2018-0001

4. Hlavatý, I., Hájková, P., Krejči, L., and Čep, R. 2018. Electric resistance welding of austenitic and galvanized steel sheets. *Technical Gazette* 25(5): 1274–1277.

5. Bondarenko, O., Verbytskyi, I., Prokopets, V., Kaloshyn, O., Spitsyn, D., Ryzhakova, T., and Kozhushko, Y. 2017. Modular power supply for micro resistance welding. *Electr. Control Commun. Eng*. 12(1): 20–26. DOI: 10.1515/ecce-2017-0003

6. Karagöz, İ. 2014. Termoplastiklerin sürtünme karıştırma kaynağı ile birleştirilmesi. PhD diss., Marmara University.

7. Jafrey, D. D., and Panneerselvam, K. 2018. Experimental investigation of resistance welded polypropylene nanocomposite joints. *J. Adhes. Sci. Technol*. 32(21): 2350–2363. DOI: 10.1080/01694243.2018.1478601

8. Xiong, X., Zhao, P., Ren, R., Zhang, Z., Cui, X., and Ji, S. 2020. Enhanced resistance-welding hybrid joints of titanium alloy/thermoplastic composites using a carbon-nanotube lamina. *Diamond and Relat. Mater.* DOI: 10.1016/j.diamond.2019.107611

9. Kim, D., Bang, J., Lee, W., Ha, I., Lee, J., Eom, H., Kim, M., Park, J., Choi, J., Kwon, J., Han, S., Park, H., Lee, D., and Ko, S. H. 2020. Highly stretchable and oxidation-resistive Cu nanowire heater for replication of the feeling of heat in a virtual world. *J. Mater. Chem. A* 8: 8281–8291. DOI: 10.1039/d0ta00380h

10. Farahani, R. D., and Dube, M. 2017. Novel heating elements for induction welding of carbon fiber/polyphenylene sulfide thermoplastic composites. *Adv. Eng. Mater.* 19(11). DOI: 10.1002/adem.201700294

11. Xiong, X., Wang, D., Wei, J., Zhao, P., Ren, R., Dong, J., and Cui, X. 2021. Resistance welding technology of fiber reinforced polymer composites: A review. *J. Adhes. Sci. Technol*. 35(15): 1593–1619. DOI: 10.1080/01694243.2020.1856514

12. Ageorges, C., and Ye, L. 2001. Simulation of impulse resistance welding for thermoplastic matrix composites. *Appl. Compos. Mater.* 8: 133–147. DOI: 10.1023/A:1011229120375

13. Ageorges, C., Ye, L., and Hou, M. 2000. Experimental investigation of the resistance welding of thermoplastic-matrix composites. Part II: Optimum processing window and mechanical performance. *Compos. Sci. Technol*. 60: 119–120.

14. Starrov, D., and Bersee, H. E. N. 2005. Resistance welding of thermoplastics composites — An overview. *Composites Part A* 36(1): 39–54. DOI: 10.1016/j.compositesa.2004.06.030

15. Talbot, É., Hubert, P., Dubé, M., and Yousefpour, A. 2011. Optimization of thermoplastic composites resistance welding parameters based on transient heat transfer finite element modelling. *J. Thermoplast. Compos. Mater.* 26(5): 699–717. DOI: 10.1177/0892705711428657

16. Troughton, M. 2008. *Handbook of Plastic Joining*. 2nd Edition, Norwich: William Andrew Inc., New York, N.Y., pp. 105–112.

17. Panneerselvam, K., Aravindan, S., and Haq, A. N. 2012. Study on resistance welding of glass fiber reinforced thermoplastic composites. *Mater. & Des*. 41: 453–459. DOI: 10.1016/j.matdes.2012.05.025

18. Villegas, I. F., and Rubio, P. V. 2015. On avoiding thermal degradation during welding of high-performance thermoplastic composites to thermoset composites. *Composites Part A* 77: 172–180. DOI: 10.1016/j.compositesa.2015.07.002

19. O'Shaughnessey, P. G., Dubé, M., and Villegas, I. F. 2016. Modelling and experimental investigation of induction welding of thermoplastic composites and comparison with other welding processes. *J. Compos. Mater.* 50(21): 2895–2910. DOI: 10.1177/0021998315614991

20. Zammar, I. A., Mantegh, I., Huq, M. S., Yousefpour, A., and Ahmadi, M. 2015. Intelligent thermal control of resistance welding of fiberglass laminates for automated manufacturing. *IEEE: ASME Transactions on Mechatronics* 20(3): 1069–1078. DOI: 10.1109/TMECH.2014.2366100

21. Benatar, A. 2016. Plastics joining. *Applied Plastics Engineering Handbook Processing, Materials, and Applications,* 2nd Ed., Ed. M. Kutz. Amsterdam, Netherlands: Elsevier.

22. Warren, K. C., Lopez-Anido, R. A., Freund, A. L., and Dagher, H. J. 2016. Resistance welding of glass fiber reinforced PET: Effect of weld pressure and heating element geometry. *J. Reinf. Plast. Compos*. 35(12): 974–985. DOI: 10.1177/0731684416633516

23. Dubé, M., Hubert, A., Yousefpour, A., and Denault, J. 2009. Fatigue failure characterisation of resistance-welded thermoplastic composites skin/stringer joints. *Int. J. Fatigue* 31(4): 719–725. DOI: 10.1016/j.ijfatigue.2008.03.012

24. Shi, H., Villegas, I. F., and Bersee, H. E. N. 2015. A displacement-detection based approach for process monitoring and processing window definition of resistance welding of thermoplastic composites. *Composites Part A* 74: 1–9. DOI: 10.1016/j.compositesa.2015.03.002

25. Ageorges, C., Ye, L., and Hou, M. 2000. Experimental investigation of the resistance welding for thermoplastic-matrix composites. Part I: Heating element and heat transfer. *Compos. Sci. Technol*. 60(7): 1027–1039. DOI: 10.1016/S0266-3538(00)00005-1

26. Hou, M., Yang, M., Beehag, A., Mai, Y. W., and Ye, L. 1999. Resistance welding of carbon fibre reinforced thermoplastic composite using alternative heating element. *Compos. Struct*. 47(1–4): 667–672. DOI: 10.1016/S0263-8223(00)00047-7

27. Shahmiri, H., Movahedi, M., and Kokabi, A. H. 2017. Friction stir lap joining of aluminium alloy to polypropylene sheets. *Sci. Technol. Weld. Joining* 22(2): 120–126. DOI: 10.1080/13621718.2016.1204171

28. Zammar, I., Huq, M. S., Mantegh, I., Yousefpour, A., and Ahmadi, M. 2017. A three-dimensional transient model for heat transfer in thermoplastic composites during continuous resistance welding. *Adv. Manuf. Polym. Compos. Sci.* 3(1): 32–41. DOI: 10.1080/20550340.2017.1311094

29. Dong, P. 2005. Residual stresses and distortions in welded structures: A perspective for engineering applications. *Sci. Technol. Weld. Joining* 10(4): 389–398. DOI: 10.1179/174329305X29465

30. Karagöz, İ., and Öksüz, M. 2018. Microstructures occurring in the joined thermoplastics sheets with friction stir welding. *J. Fac. Eng. Archit. Gazi Univ.* 33(2): 503–515. DOI: 10.17341/gazimmfd.416359

31. Hagglund, F., Spicer, M. A., and Troughton, M. 2011. Development and validation of an automated non-destructive evaluation (NDE) approach for testing welded joints in plastic pipes. *Non-Destr. Test.* 53(4): 201–213. DOI: 10.1784/insi.2011.53.4.201

32. Ungethüm, T., Spaniol, E., Hertel, M., and Füssel, U. 2020. Analysis of metal transfer and weld geometry in hot-wire GTAW with indirect resistive heating. *Weld. in the World* 64: 2109–2117. DOI:10.1007/s40194-020-00986-0

33. Dubé, M., Chazerain, A., Hubert, P., Yousefpour, A., and Bersee, H. E. N. 2013. Characterization of resistance-welded thermoplastic composite double-lap joints under static and fatigue loading. *J. Thermoplast. Compos. Mater.* 28(6): 762–776. DOI: 10.1177/0892705713490714

34. Ahmed, T. J., Stavrov, D., Bersee, and H. E. N. 2006. An experimental investigation into resistance and induction welding for aerospace structures: A comparison. *47th AIAA/ASME/ASCE/AHS/ASC Structures, Structural Dynamics and Materials Conference*, 7765–7774, Newport, R.I. DOI: 10.2514/6.2006-2245

**HÜSEYIN BAKIRCI** is with the Department of Polymer Engineering, Institute of Science, Yalova University, Yalova, Turkey. **İDRIS KARAGÖZ** (*idris.karagoz@yalova.edu.tr*) and **MEHMET ARIF KAYA** are with the Department of Polymer Materials Engineering, Faculty of Engineering, Yalova University, Yalova, Turkey.